



ELSEVIER

9 November 1995

PHYSICS LETTERS B

Physics Letters B 362 (1995) 23–28

# Chiral dynamics and the $S_{11}(1535)$ nucleon resonance <sup>★</sup>

N. Kaiser, P.B. Siegel<sup>1</sup>, W. Weise*Physik Department, Technische Universität München,  
Institut für Theoretische Physik, D-85747 Garching, Germany*

Received 27 July 1995; revised manuscript received 13 September 1995

Editor: C. Mahaux

## Abstract

The  $SU(3)$  chiral effective lagrangian at next-to-leading order is applied to the S-wave meson-baryon interaction in the energy range around the  $\eta N$  threshold. A potential is derived from this lagrangian and used in a coupled channel calculation of the  $\pi N$ ,  $\eta N$ ,  $KA$ ,  $K\Sigma$  system in the isospin- $\frac{1}{2}$ ,  $l = 0$  partial wave. Using the same parameters as obtained previously from a fit to the low energy  $\bar{K}N$  data it is found that a quasi-bound  $K\Sigma$ - $KA$ -state is formed, with properties remarkably similar to the  $S_{11}(1535)$  nucleon resonance. In particular, we find a large partial decay width into  $\eta N$  consistent with the empirical data.

PACS: 14.20.Gk; 14.40.Aq; 14.20.Jn

Keywords: Chiral dynamics; Coupled channel S-matrix; Nucleon resonances; Eta meson production; Kaon-hyperon bound state

The nucleon resonance  $S_{11}(1535)$  has the outstanding property of a very strong  $\eta N$  decay channel. The proper understanding of the low energy eta-nucleon interaction and threshold eta production consequently hinges on a correct description of the  $S_{11}(1535)$  resonance. Recently precise eta photoproduction data off protons close to threshold have become available. At MAMI (Mainz) [1] very precise angular distributions for the reaction  $\gamma p \rightarrow \eta p$  have been measured from threshold at 707 MeV up to 800 MeV photon lab energy. Together with an analogous electroproduction experiment performed at ELSA (Bonn) [2] the data cover the whole range of the  $S_{11}(1535)$  resonance. The measured cross sections clearly exhibit the strong  $S_{11}(1535)$  dominance of near threshold  $\eta$ -production.

Certainly, these new data demand a closer look at this particular nucleon resonance.

The traditional picture of the  $S_{11}(1535)$  is that of an excited three quark nucleon resonance, with one of three quarks orbiting in an  $l = 1$  state around the other two. This approach has however difficulties in explaining the large (30%–55%)  $\eta N$  branching ratio. In [3,4] the tensor force due to one-gluon exchange can produce the required state mixing to cause a large coupling to the  $\eta N$  channel for the  $S_{11}(1535)$  and a near-zero coupling for the  $S_{11}(1650)$ . However, then there are problems in reproducing the observed total decay width.

At present a frequently used ansatz for incorporating the  $S_{11}(1535)$  resonance into the  $\pi N$ ,  $\eta N$  (and  $\gamma N$ ) system is to couple these channels directly to the  $S_{11}(1535)$  via a phenomenological isobar model [5,6] with background terms [7,8]. In these models,

<sup>★</sup> Work supported in part by BMBF and GSI.

<sup>1</sup> On sabbatical leave from California State Polytechnic University, Pomona, CA 91768, USA.

the coupling constants  $g_{\pi NN^*}$  and  $g_{\eta NN^*}$  are treated as free parameters. Their values vary in the literature, but always  $g_{\eta NN^*}$  is the larger of the two. The physical reason behind the large  $\eta N$  coupling of the  $S_{11}(1535)$  is not well understood.

In this letter, we investigate the possibility that the  $S_{11}(1535)$  is a quasi-bound meson-baryon S-wave resonance. The basis of our calculation is the  $SU(3)$  chiral effective lagrangian, with explicit symmetry breaking due to the non-vanishing up, down and strange quark masses properly incorporated. This approach successfully describes the  $\Lambda(1405)$  resonance as a quasi-bound  $\bar{K}N$  state [9]. Using the same lagrangian parameters as determined from our  $\bar{K}N$  analysis, we extend the formalism to the energy range  $1.45 \text{ GeV} < \sqrt{s} < 1.6 \text{ GeV}$  to explore whether any  $S_{11}$  resonances can be formed, and what their properties are. Indeed, we find a resonant state with a large  $\eta N$  decay width as well as other characteristic properties of the  $S_{11}(1535)$ .

The effective chiral lagrangian for meson-baryon interaction can be systematically expanded in powers of small external momenta [10]

$$\mathcal{L} = \mathcal{L}^{(1)} + \mathcal{L}^{(2)} + \dots, \quad (1)$$

where the superscript denotes the power of the meson momentum. In the heavy baryon mass formalism, the leading piece at order  $q$  reads

$$\mathcal{L}^{(1)} = \text{tr}(\bar{B}i\nu \cdot DB), \quad (2)$$

with the chiral covariant derivative  $D^\mu B = \partial^\mu B + [\Gamma^\mu, B]$ , where  $B$  denotes the  $SU(3)$  baryon octet fields. This part of the lagrangian is referred to as the current algebra term. At next order in the expansion scheme,  $q^2$ , there is a host of new terms allowed by chiral symmetry. In the heavy baryon formalism the most general form relevant to S-wave scattering is given by [9]

$$\begin{aligned} \mathcal{L}^{(2)} = & \frac{1}{2M_0} \text{tr}(\bar{B}((v \cdot D)^2 - D^2)B) \\ & + b_D \text{tr}(\bar{B}\{\chi_+, B\}) + b_F \text{tr}(\bar{B}[\chi_+, B]) \\ & + b_0 \text{tr}(\bar{B}B)\text{tr}(\chi_+) + 2\{d_D \text{tr}(\bar{B}\{(v \cdot A)^2, B\}) \\ & + d_F \text{tr}(\bar{B}[(v \cdot A)^2, B]) + d_0 \text{tr}(\bar{B}B)\text{tr}((v \cdot A)^2) \\ & + d_1 \text{tr}(\bar{B}v \cdot A)\text{tr}(v \cdot AB) + d_2 \text{tr}(\bar{B}v \cdot ABv \cdot A)\}. \end{aligned} \quad (3)$$

Here  $A_\mu = -\partial_\mu \phi / 2f$  is the derivative of the octet matrix of pseudoscalar meson fields and  $f = (92.4 \pm 0.3) \text{ MeV}$  [11] is the pion decay constant. The first term above is a relativistic correction involving the baryon mass in the chiral limit,  $M_0 \simeq 0.9 \text{ GeV}$ . The parameters  $b_D = 0.066 \text{ GeV}^{-1}$  and  $b_F = -0.213 \text{ GeV}^{-1}$  are determined from the mass splittings in the baryon octet. The other six parameters have been determined in a fit to the low energy  $\bar{K}N$  experimental data [9], constrained by  $\pi N$  and  $KN$  data.

In order to investigate the possibility of resonance formation, one needs a non-perturbative approach which resums a set of diagrams to all orders. Since this leads necessarily beyond the systematic expansion scheme of chiral perturbation theory, we use a potential model. A pseudo-potential is constructed such that in the Born approximation it has the same S-wave scattering length as the effective chiral lagrangian, at order  $q^2$  (see [9] for details).

As in [9] we examine two ways of parameterizing the finite range of the potential: a local potential and one separable in the incoming and outgoing center-of-mass momenta. The local potential between channels  $i$  and  $j$  is chosen to have a Yukawa form

$$V_{ij}(\mathbf{r}) = \frac{C_{ij}\alpha_{ij}^2}{8\pi f^2} \sqrt{\frac{M_i M_j}{s\omega_i \omega_j}} \frac{\exp(-\alpha_{ij}r)}{r}, \quad (4)$$

where the indices  $i, j \in \{1, 2, 3, 4\}$  label the four channels  $\pi N$ ,  $\eta N$ ,  $K\Lambda$  and  $K\Sigma$ , respectively.  $M_i$  and  $\omega_i$  stand for the baryon mass and reduced meson-baryon energy in channel  $i$ ,  $s$  is the squared center-of-mass total energy. The parameters  $\alpha_{ij}$  can be interpreted as average ‘‘effective masses’’ representing the spectrum of exchanged particles in the  $t$ -channel mediating the interaction. The relative interaction strengths  $C_{ij}$  which follow directly from the effective chiral lagrangian are listed in the appendix.

The potential of Eq. (4) is then inserted into the coupled channel Schrödinger equation

$$(\nabla^2 + k_i^2)\psi_i = 2\omega_i \sum_{j=1}^4 V_{ij}\psi_j \quad (5)$$

to solve for the multi-channel S-matrix. For comparison we also examine a separable potential in momentum space,

Table 1

The energy of the  $K\Sigma$ - $K\Lambda$  ( $I = \frac{1}{2}$ ) quasi-bound state produced from the current algebra term alone versus the range parameter  $\alpha$

Local potential		Separable potential	
$\alpha$ (MeV)	energy	$\alpha$ (MeV)	energy
520	1604	710	1604
550	1550	750	1556
575	1489	760	1501

$$\begin{aligned} \tilde{V}_{ij}(k_i, k_j) \\ = C_{ij} \sqrt{\frac{M_i M_j}{s\omega_i \omega_j}} \frac{\alpha_i^2 \alpha_j^2}{4\pi^2 f^2 (\alpha_i^2 + k_i^2) (\alpha_j^2 + k_j^2)}, \end{aligned}$$

which is iterated in a Lippmann-Schwinger equation as described in [9].

It is instructive first to discuss qualitative aspects of the calculation. The situation at energies near the  $K\Sigma$  threshold is similar to the case near the  $\bar{K}N$  threshold investigated in [9]. There the  $\Lambda(1405)$  resonance can be produced as a quasi-bound  $\bar{K}N$  state resulting from the strong  $I = 0$  attraction between the anti-kaon and the nucleon, as well as between the pion and sigma hyperon. This attractive interaction comes at leading order  $q$  from the current algebra term, Eq. (2). In the  $S_{11}$ -channel there are several important features:

- There is a strong attraction between the kaon and sigma (see the large negative coefficient  $C_{44}$ ). Thus, as soon as the inverse range parameter  $\alpha$  exceeds a certain minimal value, a bound state will be necessarily formed below the  $K\Sigma$  threshold.
- The direct interaction between the  $\eta$  meson and the nucleon is very weak and there is a small direct coupling between the  $\pi N$  and  $\eta N$  channels ( $C_{22}$  and  $C_{12}$  are small).
- However, there is a strong coupling of both the  $\pi N$  and  $\eta N$  channels to the  $K\Sigma$  channel ( $C_{14}$  and  $C_{24}$  are sizeable).
- Thus the resonance formed will strongly connect the  $\pi N$  and  $\eta N$  channels through the coupled channel dynamics.

Let us for the moment consider only the current algebra piece, i.e., all  $b$ - and  $d$ -parameters are zero and the  $1/M_0$  corrections are neglected. In this case  $C_{22} = C_{12} = 0$ , but  $C_{23}$  and  $C_{24}$  are large. In Table 1 we show the resonance energy versus  $\alpha$  for both the local and separable potential using a common inverse range  $\alpha$

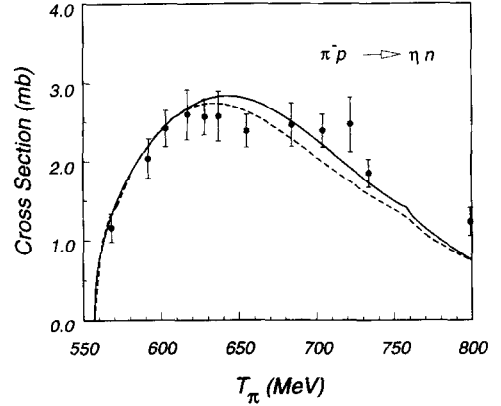


Fig. 1. The cross section  $\sigma(\pi^- p \rightarrow \eta n)$  versus the pion lab kinetic energy  $T_\pi$ . The selected data are taken from [16]. The solid/dashed line corresponds to the local/separable potential form.

for all channels. The resonance position is identified when an eigenphase of the multi-channel  $S$ -matrix is equal to  $90^\circ$ . Thus, if  $\alpha > 490$  MeV for the local potential (or 670 MeV for the separable one) a resonance is necessarily formed below the  $K\Sigma$  threshold from the current algebra piece alone. Experimentally, there are two  $S_{11}$  nucleon resonances in this energy range, at 1535 and 1650 MeV. Since only the  $S_{11}(1535)$  has a large  $\eta N$  branching ratio it is the candidate for this dynamically generated resonance.

Next we include all order  $q^2$  terms using values of the  $b$ - and  $d$ -parameters as previously obtained from a fit to the low energy  $\bar{K}N$  data and allow for a  $\pm 5\%$  uncertainty in the parameters. Thus the only free parameters are the  $\alpha_{ij}$  in Eq. (4). Since the  $\pi N$  channel is far above its threshold a satisfactory fit to all the data using only one common range for all channels could not possibly be expected. However, a good fit was found using only two range parameters: one for the  $\pi N$  channel, and one common range for the other three. The off-diagonal ranges were taken to be  $\alpha_{ij} = \frac{1}{2}(\alpha_i + \alpha_j)$ .

We performed a coupled channel calculation for the  $\pi N$   $S_{11}$  phase shift and inelasticity, as well as the  $\pi^- p \rightarrow \eta n$  cross section. The results of the fit for both the local and separable potential forms are shown in Figs. 1 and 2a, 2b. Here the range parameters are  $\alpha_{\pi N} = 320$  MeV and  $\alpha_{\eta N} = \alpha_{K\Lambda} = \alpha_{K\Sigma} = 530$  MeV for the local potential. For the separable potential the range parameters are  $\alpha_{\pi N} = 573$  MeV and  $\alpha_{K\Sigma} = 776$

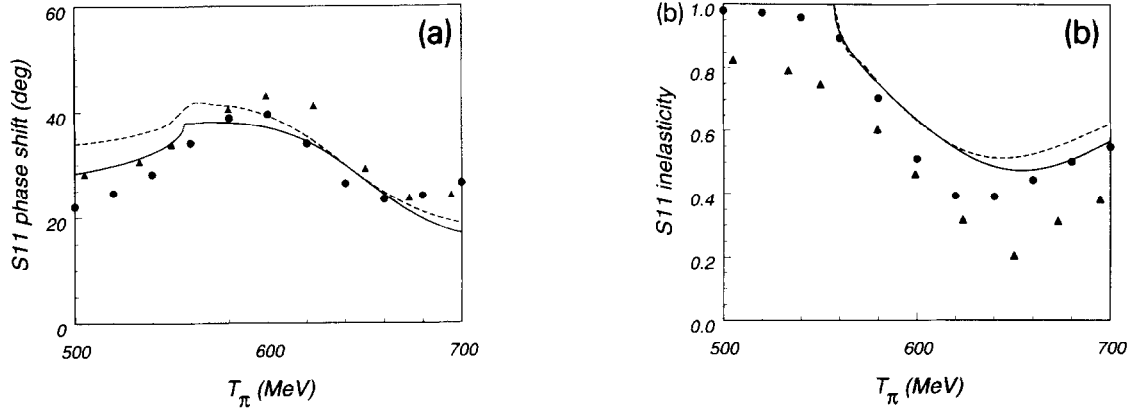


Fig. 2. (a) The pion-nucleon  $S_{11}$  phase shift as a function of the pion lab kinetic energy. The triangles/circles are from the phase shift analysis of [13]/ [14]. The full/dashed curve corresponds to a calculation using a local/separable potential form. (b) The pion-nucleon  $S_{11}$  inelasticity as a function of the pion lab kinetic energy. The notation is the same as in (a).

Table 2

Values of the lagrange parameters in units of  $\text{GeV}^{-1}$ . The inverse ranges  $\alpha$  are given in  $\text{GeV}$

Potential	$b_0$	$d_0$	$d_D$	$d_F$	$d_1$	$d_2$	$\alpha_{\pi N}$	$\alpha_{K\Sigma}$
local	-0.517	-0.68	-0.02	-0.28	+0.22	-0.41	0.32	0.53
separable	-0.279	-0.42	-0.23	-0.41	+0.27	-0.65	0.57	0.77

MeV. The values of  $b_0$  and the  $d$  parameters, which differ by only 5% from [9], are listed in Table 2.

It is remarkable that such a good fit to the  $\pi N$   $S_{11}$  phase shift and the  $\eta$ -production cross section is obtained with only two free parameters. Clearly, one can not expect the  $S_{11}$  inelasticity to be accurate since the  $\pi\pi N$  channel is neglected here. Nevertheless, this picture of the  $S_{11}(1535)$  as a dynamic resonance based on the effective chiral lagrangian reproduces many of its properties. For example we obtain a resonance mass  $M^* = 1557$  MeV and a full width  $\Gamma_{\text{tot}} = 179$  MeV. These values agree favorably with existing empirical determinations [11,1]. As byproduct we extract the  $\eta N$  S-wave scattering length to be  $a_{\eta N} = (0.68 + i0.24)$  fm. This number is close to values found from other analyses [12,8,4].

In the case of a pure Breit-Wigner resonance the  $T$ -matrix has the following energy dependence (on  $W = \sqrt{s}$ ):

$$T(W) = \frac{1}{2(M^* - W) - i\Gamma(W)} \begin{pmatrix} \gamma_1 & \sqrt{\gamma_1\gamma_2} \\ \sqrt{\gamma_1\gamma_2} & \gamma_2 \end{pmatrix}. \quad (6)$$

The constant  $M^*$  is the resonance mass and  $\Gamma(W)$  the (energy dependent) width. For a S-wave resonance which decays into two-particle final states unitarity requires the energy dependence of the width to be  $\Gamma(W) = \gamma_1 k_1(W) + \gamma_2 k_2(W)$ . Here,  $k_i(W)$  is the center-of-mass momentum in channel  $i$  and the constants  $\gamma_i$  are related to the partial decay widths  $\gamma_i k_i(M^*)$ . For a pure Breit-Wigner resonance, one eigenphase of the  $S$ -matrix (background) is zero and the other one (resonant) has the energy dependence  $\tan \delta_{\text{res}}(W) = \Gamma(W)/2(M^* - W)$ . In Fig. 3 we plot both the resonant and non-resonant eigenphases versus pion lab kinetic energy for our calculation. The dots correspond to a Breit-Wigner form with parameters  $M^* = 1557$  MeV,  $\gamma_\pi = 0.26$  and  $\gamma_\eta = 0.25$ . These numbers result in partial decay widths  $\Gamma_\pi = 124$  MeV and  $\Gamma_\eta = 55$  MeV. The branching ratio  $b_\eta = 0.31$  is still compatible with the existing analysis [11] whereas  $b_\pi = 0.69$  is somewhat too large, presumably due to the neglect of the  $\pi\pi N$  channel and our way of extracting  $\gamma_i$ . Here, the  $\gamma_i$  are determined from the energy dependence of the resonant eigenphase. For a pure Breit-Wigner resonance the ra-

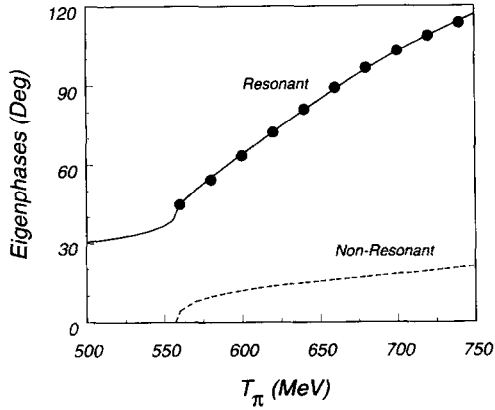


Fig. 3. The eigenphases of the multi-channel  $S$ -matrix below the  $K\Lambda$ -threshold.

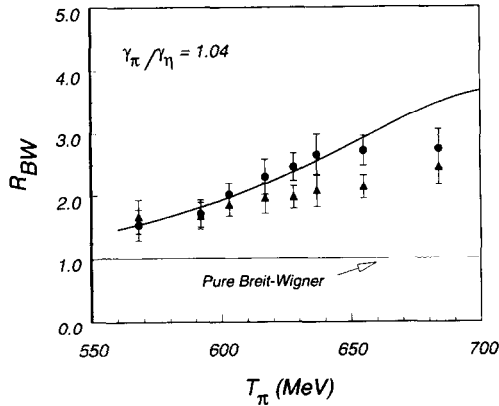


Fig. 4. The ratio  $R_{BW}$  defined in Eq. (7). The notation is the same as in Fig. 2a. The error bars reflect only those of the  $\eta$  production cross sections.

tio  $R_{BW} = \gamma_1 k_1(W) \sigma_{21}(W) / \gamma_2 k_2(W) \sigma_{11}(W)$  with  $\sigma_{21}(W) / \sigma_{11}(W)$  the ratio of cross sections for scattering from channel  $1 \rightarrow 2$  divided by that for elastic scattering ( $1 \rightarrow 1$ ) is exactly one. Any deviation from unity originates from the background eigenphase. In Fig. 4 we plot the quantity

$$R_{BW} = \frac{\gamma_\pi k_\pi \sigma(\pi N \rightarrow \eta N, S_{11})}{\gamma_\eta k_\eta \sigma(\pi N \rightarrow \pi N, S_{11})}, \quad (7)$$

which involves  $S_{11}$  partial wave cross sections only. The solid line corresponds to the potential model used here. Since the  $\eta$ -production near threshold is strongly S-wave dominated, one can identify  $\sigma(\pi N \rightarrow \eta N, S_{11})$  with  $\frac{3}{2} \sigma(\pi^- p \rightarrow \eta n)$ . The  $S_{11}$  component of the elastic  $\pi N$  cross section is con-

structed from the partial wave analysis of [13,14]. Since presently the branching ratios  $b_\pi, b_\eta$  have large uncertainties, we choose for reasons of comparison the value  $\gamma_\pi / \gamma_\eta = 1.04$  as obtained here. It is visible that  $R_{BW}$  deviates from unity which indicates that background effects (corresponding to a non-resonant eigenphase) are not negligible. In [8] a similar phenomenon was observed in so far as the coupling constants of the resonance depended strongly on the treatment of the background (nonresonant) amplitude. Also in [15] the coupling constants of the  $S_{11}(1535)$  had to be varied up to 20% from the values obtained from the widths in order to obtain a good fit to the scattering data.

In summary, we have used the  $SU(3)$  chiral effective lagrangian at next-to-leading order to investigate the possibility that the  $S_{11}(1535)$  resonance is a quasi-bound  $K\Sigma$ - $K\Lambda$  state. Using the same parameters as obtained from fitting the low energy  $\bar{K}N$  data and two finite range parameters, a resonance can be formed at 1557 MeV with the characteristic properties of the  $S_{11}(1535)$ . The  $\pi N$   $S_{11}$  phase shifts and inelasticities as well as the  $\eta N$ -production cross section are remarkably well reproduced. The dynamically generated resonance has a full width of 179 MeV and branching ratios extracted from the shape of the resonance of 69% into  $\pi N$  and 31% into  $\eta N$  final states. Furthermore, we elaborated on the background effects in the reactions dominated by the  $S_{11}(1535)$  and proposed as a measure for them the ratio  $R_{BW}$  in Eq. (7).

## Appendix

Here we list the expressions of the relative coupling strengths  $C_{ij}$  in the  $I = \frac{1}{2}$  basis entering the potential of Eq. (4). The indices 1, 2, 3, 4 refer to the  $\pi N$ ,  $\eta N$ ,  $K\Lambda$ ,  $K\Sigma$  channel, respectively, and  $E$  denotes the center-of-mass meson energy.

$$C_{11} = -E_\pi + \frac{1}{2M_0} (m_\pi^2 - E_\pi^2) + 2m_\pi^2 (b_D + b_F + 2b_0) - E_\pi^2 (d_D + d_F + 2d_0),$$

$$C_{12} = 2m_\pi^2 (b_D + b_F) + E_\pi E_\eta (d_2 - d_D - d_F),$$

$$\begin{aligned}
C_{13} &= \frac{3}{8}(E_\pi + E_K) + \frac{3}{16M_0}(E_\pi^2 - m_\pi^2 + E_K^2 - m_K^2) \\
&\quad - \frac{1}{2}(m_K^2 + m_\pi^2)(b_D + 3b_F) \\
&\quad + \frac{1}{2}E_\pi E_K(d_D + 3d_F - d_2), \\
C_{14} &= -\frac{1}{8}(E_\pi + E_K) \\
&\quad - \frac{1}{16M_0}(E_\pi^2 - m_\pi^2 + E_K^2 - m_K^2) \\
&\quad + \frac{1}{2}(b_F - b_D)(m_\pi^2 + m_K^2) \\
&\quad + \frac{1}{2}E_\pi E_K(d_D - d_F - 2d_1 - 3d_2), \\
C_{22} &= \frac{16}{3}m_K^2(b_D - b_F + b_0) \\
&\quad + 2m_\pi^2(\frac{5}{3}b_F - b_D - \frac{2}{3}b_0) \\
&\quad + E_\eta^2(d_F - \frac{5}{3}d_D - 2d_0 + \frac{2}{3}d_2), \\
C_{23} &= \frac{3}{8}(E_\eta + E_K) \\
&\quad + \frac{3}{16M_0}(E_K^2 - m_K^2 + E_\eta^2 - m_\eta^2) \\
&\quad + (b_D + 3b_F)(\frac{5}{6}m_K^2 - \frac{1}{2}m_\pi^2) \\
&\quad - E_\eta E_K(\frac{1}{2}d_F + \frac{1}{6}d_D + d_1 + \frac{5}{6}d_2), \\
C_{24} &= \frac{3}{8}(E_\eta + E_K) \\
&\quad + \frac{3}{16M_0}(E_K^2 - m_K^2 + E_\eta^2 - m_\eta^2) \\
&\quad + (\frac{5}{2}m_K^2 - \frac{3}{2}m_\pi^2)(b_F - b_D) \\
&\quad + \frac{1}{2}E_\eta E_K(d_D - d_F - d_2), \\
C_{33} &= (\frac{10}{3}b_D + 4b_0)m_K^2 + E_K^2(\frac{2}{3}d_2 - 2d_0 - \frac{5}{3}d_D), \\
C_{34} &= 2m_K^2 b_D + E_K^2(d_2 - d_D), \\
C_{44} &= -E_K - \frac{1}{2M_0}(E_K^2 - m_K^2) \\
&\quad + 2m_K^2(b_D - 2b_F + 2b_0) \\
&\quad + E_K^2(2d_F - d_D - 2d_0).
\end{aligned}$$

## References

- [1] B. Krusche et al., Phys. Rev. Lett. 74 (1995) 3736.
- [2] B. Schoch, Prog. Part. Nucl. Phys. 35 (1995) 43.
- [3] R. Koniuk and N. Isgur, Phys. Rev. D 21 (1980) 1868; N. Isgur and G. Karl, Phys. Lett. B 72 (1977) 109.
- [4] M. Arima, K. Shimizu and K. Yazaki, Nucl. Phys. A 543 (1993) 613.
- [5] R.S. Bhalerao and L.C. Liu, Phys. Rev. Lett. 54 (1985) 865.
- [6] C. Bennhold and H. Tanabe, Nucl. Phys. A 350 (1991) 625.
- [7] M. Benmerrouche and N.C. Mukhopadhyay, Phys. Rev. Lett. 67 (1991) 1070.
- [8] Ch. Sauermann, B.L. Friman and W. Nörenberg, Phys. Lett. B 341 (1995) 261.
- [9] N. Kaiser, P.B. Siegel and W. Weise, Chiral Dynamics and the Low Energy Kaon Nucleon Interaction, Nucl. Phys. A (1995), in print.
- [10] For some recent reviews see, G. Ecker, Prog. Part. Nucl. Phys. 35 (1995) 1; V. Bernard, N. Kaiser and Ulf-G. Meißner, Int. J. Mod. Phys. E 4 (1995) 193.
- [11] Particle Data Group, Phys. Rev. D 50 (1994) 1173.
- [12] C. Wilkin, Phys. Rev. C 47 (1993) R938.
- [13] G. Höhler, in: Landolt-Börnstein, Vol. 9b2, ed. H. Schopper (Springer, Berlin, 1983).
- [14] R. Arndt et al., SAID computer program (Virginia Polytechnic Institute and State University, Blacksburg, VA 24061).
- [15] H.C. Chiang, E. Oset and L.C. Liu, Phys. Rev. C 44 (1991) 738.
- [16] M. Clajus and B.M.K. Nefkens,  $\pi N$  Newsletter 7 (1992) 76; the original data are taken from W. Deinet et al., Nucl. Phys. B 11 (1969) 495; F. Bulos et al., Phys. Rev. 187 (1969) 1827; W.B. Richards et al., Phys. Rev. D 1 (1970) 10.